

# Modeling Thin Graphene Sheets in the WLP-FDTD Algorithm with Surface Boundary Condition

Wei-Jun Chen, Qi-Wen Liang\*, Shi-Yu Long, and Min Zhao

**Abstract**—In this article, a two-dimensional (2D) unconditionally stable finite-difference time-domain (FDTD) approach is proposed for graphene electromagnetic (EM) device simulation. The weighted Laguerre polynomials (WLPs) are utilized to resolve stability concerns, and graphene is modelled as a thin conductive layer incorporating the surface boundary condition (SBC) in WLP-FDTD scheme. The transmittance of EM signal propagating through two graphene layers is calculated for 0–10 THz to verify the effectiveness of the proposed method. The simulation results agree excellently with the results calculated from the analytical and other numerical models. The proposed SBC-WLP-FDTD method provides an alternative numerical approach to simulate graphene-like materials with improved computing efficiency.

## 1. INTRODUCTION

The finite-difference time-domain (FDTD) algorithm has been proved to be an effective approach for graphene-based EM device simulations in the past few years [1–4]. However, the numerical modeling of these devices remains challenging due to the single-atom thickness of graphene. According to the Courant-Friedrich-Levy (CFL) stability constraint, traditional FDTD method has to utilize extra fine meshing and ultra-small time step in order to model the atomic-thick graphene. Hence, these FDTD approaches unavoidably consume large memory and computing time. To reduce the memory usage and improve computing efficiency, a hybrid algorithm known as the auxiliary differential equation weighted Laguerre polynomials (ADE-WLP) FDTD, has been proposed [5, 6]. Although it does show the advantages in memory usage and computing efficiency, a fine grid division has to be applied to the graphene layer in this method, resulting in a time-consuming sparse matrix equation. To solve this issue, the factorization splitting technique is introduced in [7], demonstrating excellent reduction in computing time. Alternatively, Nayyeri et al. proposed an FDTD method in which graphene sheet is modelled as a conductive layer, and surface boundary condition (SBC) is utilized to avoid the implementation of fine meshing [8]. However, these approaches are limited by the CFL stability constraint.

Therefore, in this article an unconditionally stable numerical approach, utilizing WLP and conductive SBC (i.e., SBC-WLP-FDTD), is presented to model graphene-based devices. The update equation of a 2D case is derived, and the transmission coefficient of EM wave propagation through graphene is calculated for 0–10 THz. The simulation results are validated with the results achieved with the analytical model and a few conventional FDTD methods. A detailed computation effort comparison between the numerical approaches is also presented.

---

*Received 15 April 2020, Accepted 7 May 2020, Scheduled 25 May 2020*

\* Corresponding author: Qi-Wen Liang (liangqiwen\_j@163.com).

The authors are with the School of Information Engineering, Lingnan Normal University, Zhanjiang 524048, China.

## 2. MATHEMATICAL FORMULATION

In this section, the detailed derivation procedure of the update equations of the proposed FDTD method is presented for a 2D case. Fig. 1 demonstrates the unit cell of a Cartesian computational grid, where graphene is represented as a conductive layer at the spatial grid  $I + 1/2$ . The magnetic field  $H_z$  and electric fields  $E_x$ ,  $E_y$  on both sides of the graphene sheet are also shown in the picture.

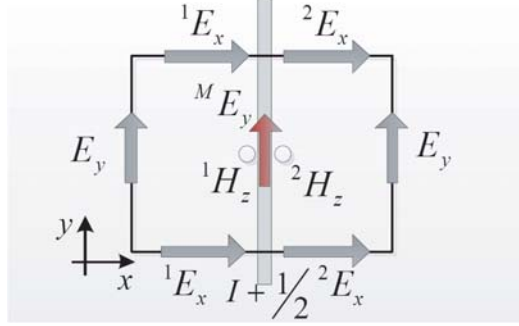


**Figure 1.** Yee cell including graphene layer of the 2-D WLP-FDTD model.

The updating equations for  $E_x$ ,  $E_y$ , and  $H_z$  can be derived by implementing  $\partial B/\partial t = -\nabla \times E$  at  $(I + 0.5, j)$  [8]:

$$\mu_1 \delta_t^c \{ {}^1 H_z \} = \delta_y^c \{ {}^1 E_x |_{I+0.5, j+0.5} \} - \delta_x^b \{ E_y |_{I+0.5, j+0.5} \} \quad (1)$$

$$\mu_2 \delta_t^c \{ {}^2 H_z \} = \delta_y^c \{ {}^2 E_x |_{I+0.5, j+0.5} \} - \delta_x^f \{ E_y |_{I+0.5, j+0.5} \} \quad (2)$$

where  $\mu_1$  and  $\mu_2$  are the permeability of materials sandwiching the graphene sheet, and  $\delta^c$ ,  $\delta^b$ , and  $\delta^f$  are defined as [8]

$$\delta_g^c \{ F \} = \frac{F(g + \Delta g/2) - F(g - \Delta g/2)}{\Delta g} \quad (3)$$

$$\delta_g^b \{ F \} = \frac{F(g) - F(g - \Delta g/2)}{\Delta g/2} \quad (4)$$

$$\delta_g^f \{ F \} = \frac{F(g + \Delta g/2) - F(g)}{\Delta g/2} \quad (5)$$

As  ${}^1 E_x$  and  ${}^1 E_y$  can be written as

$$\varepsilon_0 \delta_t^{c1} E_x |_{I+0.5, j+0.5} = \delta_y^{c1} H_z \quad (6)$$

$$\varepsilon_0 \delta_t^{c2} E_x |_{I+0.5, j+0.5} = \delta_y^{c2} H_z \quad (7)$$

where  $\varepsilon_0$  is the dielectric permittivity of free space, applying the frequency domain boundary condition at the graphene surface, we arrive at

$${}^2 H_z(\omega) - {}^1 H_z(\omega) = \sigma_s(\omega) {}^M E_y(\omega) \quad (8)$$

where  $\sigma_s$  is the surface conductivity of graphene, and  ${}^M E_y$  is the electric field at  $(I + 1/2)$ . According to Kubo's formula [9], the conductivity of graphene is composed of both intraband and interband terms. For frequency below 10 THz, the intraband term dominates, and  $\sigma_s$  can be expressed as

$$\sigma_s = \sigma_{\text{intra}}(\omega, \mu_c, \Gamma, T) = \frac{e^2 k_B T}{\pi \hbar^2 (j\omega - 2\Gamma)} \left( \frac{\mu_c}{k_B T} + 2 \ln \left( e^{-\frac{\mu_c}{k_B T}} + 1 \right) \right) \quad (9)$$

where  $e$  is the charge of an electron,  $T$  the temperature,  $\hbar$  the reduced Plank's constant,  $\Gamma$  the scattering rate,  $k_B$  the Boltzmann constant, and  $\mu_c$  the chemical potential [9]. Substituting Eq. (9) into Eq. (8) and applying the frequency to time domain transform (i.e.,  $j\omega \rightarrow \partial/\partial t$ ) yields

$$\sigma_0 {}^M E_y |_{x,y,t} = {}^2 H_z |_{x,y,t} + \tau \frac{\partial {}^2 H_z |_{x,y,t}}{\partial t} - {}^1 H_z |_{x,y,t} - \tau \frac{\partial {}^1 H_z |_{x,y,t}}{\partial t} \quad (10)$$

where  $\tau = 1/(2\Gamma)$  is the scattering time, and  $\sigma_0 = (e^2\tau k_B T/\pi\hbar^2)(\mu_c/k_B T + 2\ln(e^{-\mu_c/k_B T} + 1))$ . By using the weighted Laguerre basis functions  $\phi_p(st)$ , the field components can be rewritten as [10]

$$\{^1H_z, ^2H_z, ^M E_y, ^1E_x, ^2E_x |_{x,y,t}\} = \sum_{p=0}^{\infty} \{^1H_z^p, ^2H_z^p, ^M E_y^p, ^1E_x^p, ^2E_x^p |_{x,y}\} \phi_p(st) \quad (11)$$

where  $p$  is the order of Laguerre functions, and  $s$  is the time-scale factor. The derivative of any field  $U(x, y, t)$  in Eqs. (1), (2), (6), (7), and (10) with respect to  $t$  is

$$\frac{\partial U |_{x,y,t}}{\partial t} = s \sum_{p=0}^{\infty} \left[ 0.5U^p |_{x,y} + \sum_{k=0, p>0}^{p-1} U^k |_{x,y} \right] \phi_p(st) \quad (12)$$

Inserting Eqs. (11) and (12) into Eqs. (1), (2), (6), (7), and (10), multiplying both sides by  $\phi_p(st)$ , and integrating over  $st \in [0, \infty)$ , we have

$$\begin{aligned} ^1H_z^p |_{I+1/2, j+1/2} &= \frac{2}{\mu_1 s \Delta y} (^1E_x^p |_{I+1/2, j+1} - ^1E_x^p |_{I+1/2, j}) \\ &\quad - \frac{4}{\mu_1 s \Delta x} (^M E_y^p |_{I+1/2, j+1/2} - E_y^p |_{I, j+1/2}) - 2 \sum_{k=0, p>0}^{p-1} ^1H_z^k |_{I+1/2, j+1/2} \end{aligned} \quad (13)$$

$$\begin{aligned} ^2H_z^p |_{I+1/2, j+1/2} &= \frac{2}{\mu_2 s \Delta y} (^2E_x^p |_{I+1/2, j+1} - ^2E_x^p |_{I+1/2, j}) \\ &\quad - \frac{4}{\mu_2 s \Delta x} (E_y^p |_{I+1, j+1/2} - ^M E_y^p |_{I+1/2, j+1/2}) - 2 \sum_{k=0, p>0}^{p-1} ^2H_z^k |_{I+1/2, j+1/2} \end{aligned} \quad (14)$$

$$\begin{aligned} ^M E_y^p |_{I+1/2, j+1/2} &= \frac{1 + 0.5\tau s}{\sigma_0} ^2H_z^p |_{I+1/2, j+1/2} + \frac{\tau s}{\sigma_0} \sum_{k=0, p>0}^{p-1} ^2H_z^k |_{I+1/2, j+1/2} \\ &\quad - \frac{1 + 0.5\tau s}{\sigma_0} ^1H_z^p |_{I+1/2, j+1/2} - \frac{\tau s}{\sigma_0} \sum_{k=0, p>0}^{p-1} ^1H_z^k |_{I+1/2, j+1/2} \end{aligned} \quad (15)$$

$$^1E_x^p |_{I+1/2, j} = \frac{4}{a} (^1H_z^p |_{I+1/2, j+1/2} - ^1H_z^p |_{I+1/2, j-1/2}) - 2 \sum_{k=0, p>0}^{p-1} ^1E_x^k |_{I+1/2, j} \quad (16)$$

$$^2E_x^p |_{I+1/2, j} = \frac{4}{a} (^2H_z^p |_{I+1/2, j+1/2} - ^2H_z^p |_{I+1/2, j-1/2}) - 2 \sum_{k=0, p>0}^{p-1} ^2E_x^k |_{I+1/2, j} \quad (17)$$

Here,  $\Delta x$  and  $\Delta y$  are the edge lengths of the grid in  $x$  and  $y$  directions, respectively, and  $a = \Delta y s \varepsilon$ . Inserting Eqs. (13) and (14) into Eqs. (15)–(17), we have

$$\begin{aligned} &\left(1 + \frac{8 + 4\tau s}{\sigma_0 \mu_1 s \Delta x}\right) ^M E_y^p |_{I+1/2, j+1/2} - \frac{2 + \tau s}{\sigma_0 \mu_1 s \Delta y} (^1E_x^p |_{I+1/2, j+1} - ^1E_x^p |_{I+1/2, j}) \\ &\quad - \frac{4 + 2\tau s}{\sigma_0 \mu_1 s \Delta x} E_y^p |_{I, j+1/2} + \frac{2 + \tau s}{\sigma_0 \mu_1 s \Delta y} (^2E_x^p |_{I+1/2, j+1} - ^2E_x^p |_{I+1/2, j}) \\ &\quad - \frac{4 + 2\tau s}{\sigma_0 \mu_1 s \Delta x} E_y^p |_{I+1, j+1/2} = -\frac{2}{\sigma_0} \sum_{k=0, p>0}^{p-1} (^1H_z^k |_{I+1/2, j+1/2} - ^2H_z^k |_{I+1/2, j+1/2}) \end{aligned} \quad (18)$$

$$\begin{aligned}
& \left(1 + \frac{8}{a\mu_1 s \Delta y}\right) {}^1 E_x^p |_{I+1/2,j} - \frac{4}{a\mu_1 s \Delta y} {}^1 E_x^p |_{I+1/2,j+1} + \frac{8}{a\mu_1 s \Delta x} ({}^M E_y^p |_{I+1/2,j+1/2} - E_y^p |_{I,j+1/2}) \\
& - \frac{4}{a\mu_1 s \Delta y} {}^1 E_x^p |_{I+1/2,j-1} - \frac{8}{a\mu_1 s \Delta x} ({}^M E_y^p |_{I+1/2,j-1/2} - E_y^p |_{I,j-1/2}) \\
& = -2 \sum_{k=0,p>0}^{p-1} {}^1 E_x^k |_{I+1/2,j} - \frac{4}{a} \sum_{k=0,p>0}^{p-1} {}^1 H_z^k |_{I+1/2,j+1/2} + \frac{4}{a} \sum_{k=0,p>0}^{p-1} {}^1 H_z^k |_{I+1/2,j-1/2} \tag{19}
\end{aligned}$$

$$\begin{aligned}
& \left(1 + \frac{8}{a\mu_2 s \Delta y}\right) {}^2 E_x^p |_{I+1/2,j} - \frac{4}{a\mu_2 s \Delta y} {}^2 E_x^p |_{I+1/2,j+1} + \frac{8}{a\mu_2 s \Delta x} (E_y^p |_{I+1,j+1/2} - {}^M E_y^p |_{I+1/2,j+1/2}) \\
& - \frac{4}{a\mu_2 s \Delta y} {}^2 E_x^p |_{I+1/2,j-1} - \frac{8}{a\mu_2 s \Delta x} (E_y^p |_{I+1,j-1/2} - {}^M E_y^p |_{I+1/2,j-1/2}) \\
& = -2 \sum_{k=0,p>0}^{p-1} {}^2 E_x^k |_{I+1/2,j} - \frac{4}{a} \sum_{k=0,p>0}^{p-1} {}^2 H_z^k |_{I+1/2,j+1/2} + \frac{4}{a} \sum_{k=0,p>0}^{p-1} {}^2 H_z^k |_{I+1/2,j-1/2} \tag{20}
\end{aligned}$$

As long as the updating Equations (18)–(20) are derived at the graphene sheet, the classical matrix system for WLP-FDTD method can be revised. Thus, the electric fields can be achieved by solving Equations (18)–(20). With Eqs. (13) and (14), the magnetic fields on both sides of the graphene sheet can be calculated explicitly.

### 3. NUMERICAL RESULTS

In order to validate the effectiveness of the proposed FDTD model, we simulate the EM wave propagation through two graphene layers, and the transmission coefficients are calculated with respected to the  $TE_z$  mode. A sinusoidally modulated Gaussian pulse  $J_y(t) = \exp[-(t - T_c)^2/T_d^2] \sin[2\pi f_c(t - T_c)]$  is used as an incident signal, where  $T_d = 1/(2f_c)$ ,  $T_c = 3/(2f_c)$ , and  $f_c = 5$  THz. A finite time interval ( $T_f$ ) of  $2 \times 10^{-12}$  s as well as a time scaling factor ( $s$ ) of  $3.7699 \times 10^{14}$  is also used in the simulation. The order-marching step number ( $N$ ) used in the FDTD calculation is 148 [11]. As shown in Fig. 2, the plane wave with linear polarization in the direction of  $y$ -axis is applied perpendicularly to the surface of graphene. An air gap with the thickness of 10 nm is induced between the graphene layers. The dimension of the model is  $400 * d \times 20 * d$  where  $d = 1500$  nm, and perfect matched layers (PMLs) as absorbing boundary conditions (ABCs) are used to truncate the computational area. The conductivity of graphene is calculated with chemical potential  $\mu_c = 0.5$  eV at room temperature (i.e.,  $T = 300$  K) with a scattering time of  $\tau = 0.5 \times 10^{-12}$  s.

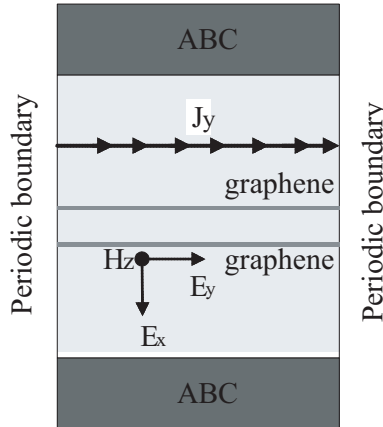


**Figure 2.** Schematic of EM wave propagation through two graphene sheets.

The ADE-FDTD, SBC-FDTD, ADE-WLP-FDTD and analytical method are also used for comparison with the proposed approach (i.e., SBC-WLP-FDTD). The ultrathin thickness of graphene results in a cell size as small as  $\Delta x = 1$  nm and  $\Delta y = 1500$  nm near the graphene layers for ADE-FDTD and ADE-WLP-FDTD. The grid size  $\Delta x$  increases gradually in the direction of  $x$ -axis while  $\Delta y$  remains constant and arrives at a maximum of  $\Delta x = 1500$  nm. The analytical solution is calculated as  $T = 1/(1 + \eta_0 \sigma_s)$ , where  $\eta$  is the free space impedance [9]. Fig. 3 illustrates the calculated results for all methods. All the curves overlap well with each other, indicating the validation of the proposed approach. Table 1 illustrates the summarized details of the numerical methods. The proposed FDTD model exhibits better computation efficiency than the other FDTD methods. The simulation results are achieved on PC with Intel i5-421M and 8 G RAM.

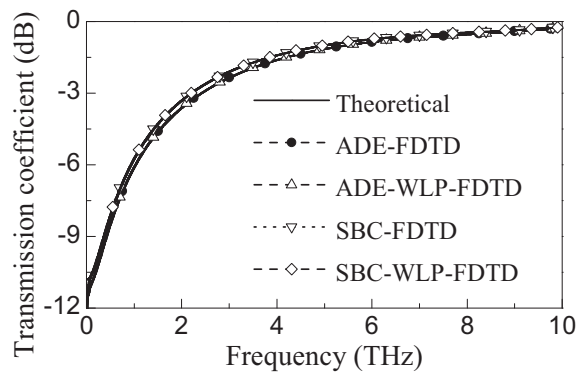


**Figure 3.** Transmission coefficient calculated with analytical and various numerical models.

**Table 1.** Comparisons of numerical approaches.

Method	$\Delta t$ (fs)	Grid cells	Marching steps	Computing time (s)
ADE-FDTD	$1.67 \times 10^{-3}$	$482 \times 20$	$9 \times 10^5$	15970
ADE-WLP-FDTD	2.5	$482 \times 20$	148	34
SBC-FDTD	$1.67 \times 10^{-2}$	$400 \times 20$	$9 \times 10^4$	411
This work	2.5	$400 \times 20$	148	16

#### 4. CONCLUSION

In summary, this work implements graphene as a conductive sheet with the implicit SBC-WLP-FDTD method to simulate graphene-based EM devices. The 2D updating equation has been derived to simulate EM wave propagation in the graphene, and simulation results have been validated against analytical calculation and three other numerical methods. As the proposed method does not require fine meshing, it demonstrates the best computing efficiency among all the numerical approaches while retains excellent computing accuracy. It provides an alternative approach for numerical device simulation involving graphene-like 2D materials with improved time efficiency.

#### ACKNOWLEDGMENT

The work is supported by the Natural Science Foundation of Guangdong province, China (No. 2018A030307077, 2019A1515010489, 2018A030307016); Innovation and strong school project of Guangdong provincial education department, China (No. 2017KTSCX116).

## REFERENCES

1. Lin, H., M. F. Pantoja, L. D. Angulo, et al., "FDTD modeling of graphene devices using complex conjugate dispersion material model," *IEEE Microw. Wireless Compon. Lett.*, Vol. 22, No. 12, 612–614, Dec. 2012.
2. Yu, X. and C. D. Sarris, "A perfectly matched layer for subcell FDTD and applications to the modeling of graphene structures," *IEEE Antennas Wireless Propag. Lett.*, Vol. 11, 1080–1083, 2012.
3. Ahmed, I., E. H. Khoo, and E. Li, "Efficient modeling and simulation of graphene devices with the LOD-FDTD method," *IEEE Microw. Wireless Compon. Lett.*, Vol. 23, No. 6, 306–308, Jun. 2013.
4. De Oliveira, R. M. S., N. R. N. M. Rodrigues, and V. Dmitriev, "FDTD formulation for graphene modeling based on piecewise linear recursive convolution and thin material sheets techniques," *IEEE Antennas Wireless Propag. Lett.*, Vol. 14, 767–770, 2015.
5. Chen, W.-J., W. Shao, J. Quan, and S.-Y. Long, "Modeling of wave propagation in thin graphene sheets with WLP-FDTD method," *Journal of Electromagnetic Waves and Applications*, Vol. 30, No. 6, 780–787, Apr. 2016.
6. Chen, W.-J. and S.-Y. Long, "Modeling of wave propagation in thin graphene sheets with 2-D ADE-WLP-FDTD method," *2016 IEEE International Conference on Microwave and Millimeter Wave Technology (ICMMT)*, Vol. 1, 434–436, Jun. 2016.
7. Zhu, Q.-Y. and W.-J. Chen, "Modeling thin graphene sheets with efficient 2-D WLP-FDTD method," *2017 Sixth Asia-Pacific Conference on Antennas and Propagation (APCAP)*, Vol. 1, Oct. 2017.
8. Nayyeri, V., M. Soleimani, and O. M. Ramahi, "Modeling graphene in the finite-difference time-domain method using a surface boundary condition," *IEEE Trans. Antennas Propag.*, Vol. 61, No. 8, 4176–4182, Aug. 2013.
9. Hanson, G. W., "Dyadic Greens functions and guided surface waves for a surface conductivity model of graphene," *J. Appl. Phys.*, Vol. 103, No. 6, Mar. 2008.
10. Chung, Y. S., T. K. Sarkar, B. H. Jung, and M. Salazar-Palma, "An unconditionally stable scheme for the finite-difference time-domain method," *IEEE Trans. Microw. Theory Tech.*, Vol. 51, No. 3, 697–704, Mar. 2003.
11. Chen, W.-J., W. Shao, J.-L. Li, and B.-Z. Wang, "Numerical dispersion analysis and key parameter selection in Laguerre-FDTD method," *IEEE Microw. Wireless Compon. Lett.*, Vol. 23, No. 12, 629–631, Dec. 2013.